THE JOURNAL OF COMPARATIVE NEUROLOGY 335:267–282 (1993)

Expiratory Neurons of the Bötzinger Complex in the Rat: A Morphological Study Following Intracellular Labeling With Biocytin

THOMAS H. BRYANT, SHIGETAKA YOSHIDA, DENIS DE CASTRO, AND JANUSZ LIPSKI
Department of Physiology, School of Medicine, University of Auckland, New Zealand

ABSTRACT

The term "Bötzinger Complex" (BOT) refers to a distinct group of neurons, located near the rostral portion of the nucleus ambiguus, which are known to play an important role in the control of respiratory movements. Previous studies conducted in cats have demonstrated that most of these neurons are active during expiration, exerting a monosynaptic inhibitory action on several subpopulations of inspiratory neurons in the medulla and spinal cord. The aim of this study was to examine morphological properties and possible synaptic targets of BOT neurons in the rat. Forty-one expiratory neurons were labeled intracellularly with biocytin; 12 were interneurons (BOT neurons) and 29 were motoneurons. The latter could not be antidromically activated following stimulation of the superior laryngeal or vagal nerves. BOT neurons showed extensive axonal arborisations in the ipsilateral medulla, with some projections to the contralateral side. Bouton-like axon varicosities mainly clustered in two areas: near the parent cell bodies, and in the area corresponding to the rostral part of the ventral respiratory group (VRG). In five pairs of labeled neurons, each consisting of one BOT neuron and one inspiratory neuron in the rostral VRG, no appositions were identified at the light microscopic level between axons of BOT neurons and dendrites or cell bodies of inspiratory neurons. These results demonstrate that some features of BOT expiratory neurons in the rat are similar to those previously described in cats. The differences include their more ventral location in relation to the compact formation of nucleus ambiguus (retrofacial nucleus), and the relative paucity in the rat of neurons displaying an augmenting pattern of activity and of neurons with spinally projecting axons. In addition, we were unable to find morphological evidence for contacts between labeled BOT neurons and ipsilateral inspiratory neurons near the obex level, a finding not consistent with previous electrophysiological studies in the cat in which such synaptic connections have been identified.

Key words: electrophysiology, nucleus ambiguus, interneurons, motoneurons, axon collaterals, rostral ventrolateral medulla, respiratory control

The rostral and ventral part of the medulla oblongata (rostral ventrolateral medulla, RVLM) is widely considered to be a key brainstem site for the integration of many autonomic and somatic functions, including the control of respiration and blood pressure (e.g., Feldman and Ellenberger, '88; Ezure, '90; Guyenet, '90). One distinct subset of these medullary neurons, often referred to as the "subretrofacial nucleus," represents an output pathway providing an excitatory drive to sympathetic preganglionic neurons (e.g., Chalmers and Pilowsky, '91; Dampney, '93). Another group, which occupies a RVLM region partially overlapping the subretrofacial nucleus (Ellenberger et al., '90a; Pilowsky et al., '90) and is known to be respiratory in function, is the Bötzinger Complex. The term Bötzinger Complex (BOT) refers to a group of propriobulbar or bulbospinal respiratory neurons, most of which are active during the expiratory phase. This contrasts with the more caudally located neurons of the adjacent portion of the ventral respiratory group (rostral VRG), most of which are active during inspiration (for reviews see Feldman, '86; Long and Duffin, '86; Ezure, '90).

Accepted April 16, 1993.

S. Yoshida's present address is Department of Neuroanatomy, Osaka University Medical School, Osaka 565, Japan.

Address reprint requests to Professor J. Lipski, Department of Physiology, University of Auckland, Private Bag 92019, Auckland, New Zealand.

Since the original description (Lipski and Merrill, '80), there has been continuing interest in BOT neurons, with numerous authors discussing the involvement of this neuronal group in the control of "normal" breathing cycles, various respiratory and nonrespiratory behaviours, and reflex responses to activation of specific respiratory afferents (Merrill et al., '83; Lipski et al., '84; Orem and Brooks, '87; Otake et al., '87; Shannon and Lindsey, '87; Bongianni et al., '88; Manabe and Ezure, '88; Speck, '89; St. John et al., '89; Jiang and Lipski, '90; Miller and Nonaka, '90; Anders et al., '91; Fukuda and Koga, '91; Chang, '92). Most studies of BOT neurons have been conducted in the cat. These include extracellular recording and tracing of axonal projections with either antidromic mapping or antero- (or retro-) grade tracers (e.g., Lipski and Merrill, '80; Bianchi and Barillot, '82; Fedorko and Merrill, '84; Otake et al., '88; Smith et al., '89; Mateika and Duffin, '89), identification of monosynaptic inhibitory connections with spike-triggered averaging or cross-correlation (e.g., Kubin and Lipski, '80; Merrill et al., '83; Merrill and Fedorko, '84, Lindsey et al., '87; Ezure and Manabe, '89; Ezure et al., '89; Fedorko et al., '89; Jiang and Lipski, '90), and intracellular labeling for examination of morphological details or immunocytochemistry (Otake et al., '87; Grélot et al., '88; Otake et al., '90; Lipski et al., '93).

In recent years, rats have been increasingly used as animal models for studying the neural control of breathing. However, in contrast to the large number of studies conducted in cats, relatively little is known about the properties of BOT neurons in the rat. In recent extracellular and intracellular studies conducted in this species, a concentration of mainly expiratory neurons was found at the rostral end of the VRG (Ezure et al., '88; Ellenberger and Feldman, '90; Pilowsky et al., '90; Zheng et al., '91a, '92) suggesting the existence of a BOT region very similar to that of the cat. However, such a conclusion may be premature as some properties of neurons in this region seem to differ between the two species. For example, the majority of BOT expiratory neurons in the cat fire with an augmenting pattern (i.e., their firing frequency increases during expiration), while recordings in the rat suggest a prevalence of neurons with a constant or decrementing pattern of firing in expiration (e.g., Ezure et al., '88; Zheng et al., '91a, '92). In addition, little is known about the medullary and other projections of BOT neurons in the rat.

Although extensive ipsi- and contralateral projections of neurons located near the rostral end of the nucleus ambiguus to the medulla and spinal cord have been reported on the basis of retrograde labeling (Ellenberger and Feldman, '90; Ellenberger et al., '90a; Núñez-Abades et al., '91), such projections have not been systematically described for electrophysiologically identified respiratory neurons (see Pilowsky et al., '90). The demonstration of medullary axonal projections is important not only for tracing synaptic connections, but also for differentiation from motoneurons located in adjacent regions (semicompact division of the nucleus ambiguus, motor nucleus of facial nerve), as studies in cats and rats have shown that these often show respiratory patterns of discharge similar to those reported for BOT neurons (e.g., Otake et al., '87; Bianchi et al., '88; Grélot et al., '88; Pilowsky et al., '90; Zheng et al., '91b, '92).

The present study was undertaken to describe the activity, the location, and some details of the cellular morphology of BOT neurons in the rat, using intracellular recording and labeling with biocytin. The choice of this label was based on recent reports which stress superior staining of fine axon collaterals and presynaptic bouton-like structures with biocytin (or a related compound, neurobiotin) compared with results normally obtained with horseradish peroxidase (e.g., Kawaguchi et al., '90; Morgan et al., '91; Jacquin et al., '92). In addition, an attempt was made to define possible synaptic targets of BOT neurons by labeling pairs of neurons, each consisting of one BOT neuron and one inspiratory neuron in the rostral portion of the VRG.

MATERIALS AND METHODS

Animal preparation

Experiments were performed on 26 male Wistar rats (350–530 g), anesthetized with sodium pentobarbital (Nembutal, 60–90 mg/kg, i.p.). Surgical anesthesia (as indicated by slow and regular central breathing and no change in heart rate or blood pressure following nociceptive stimuli) was maintained with supplementary doses of Nembutal (3–6 mg/hr, i.v.). Following tracheostomy, animals were placed in a stereotaxic frame. The dorsal surface of the medulla oblongata and cervical part of the spinal cord were exposed by occipital craniotomy, cerebellectomy, and laminectomy. The degree of ventroflexion of the head was adjusted to keep the dorsal medullary surface horizontal. The left phrenic, superior laryngeal, and vagus nerves were dissected in the neck, cut peripherally and prepared for standard bipolar recording or stimulation. In 9 experiments, the superior laryngeal and vagus nerves were dissected on both sides. Animals were paralysed with pancuronium bromide (Pavulon, 0.2–0.4 mg/hr, i.v.) and artifically ventilated with O_2-enriched air. A bilateral pneumothorax was made and an expiratory load of 3–4 cm H_2O was applied. Rectal temperature (36.5°C), arterial blood pressure (mean above 100 mm Hg), end-tidal CO_2 (range, 4.0 to 6.0%) and tracheal pressure were monitored.

Stimulation and recording

The activity of the phrenic nerve was amplified and filtered (60 Hz–3 kHz). Separate electrodes were placed on the superior laryngeal and vagus nerves for antidromic stimulation of vagal motoneurons (stimulus intensity, 0.1 ms, up to 5.0 V). Two monopolar stimulating electrodes were placed bilaterally in the ventrolateral funiculus at the junction between the C_2 and C_3 segments of the spinal cord for antidromic identification of medullary neurons projecting to the spinal cord (stimulus intensity, 0.1–0.2 ms, up to 1.0 mA). Conduction velocities of the descending axons were determined from single point antidromic activation assuming a linear axon trajectory, and are therefore subject to the errors inherent in this method (Dick and Berger, '85). In each experiment, recordings were initially made with extracellular low-impedance glass microelectrodes containing 3 M NaCl (tip diameter, 1.5–2.5 μm). A limited number of tracks (usually less than 10; spacing between tracks, 100 or 150 μm) were made mainly in the mediolateral direction, approximately 2.0 mm rostral to the obex, at a rostrocaudal level corresponding to the middle part of the column of expiratory neurons described in the rat by Ezure et al. ('88). It was possible in all experiments to locate multi-unit respiratory activity at a depth of 2.2–3.3 mm, with the discharge usually occurring during expiration (as defined by recording from the phrenic nerve). Although it was not possible at this stage to distinguish between motoneurons and interneurons (see Discussion), these re-

cordings were used as an initial guide to the position of the BOT. In addition, the location of the recordings near the rostral part of the nucleus ambiguus (cf. Hinrichsen and Ryan, '81; Bieger and Hopkins, '87; Otake et al., '87) was confirmed by antidromic field potentials evoked at that site by stimulation of the superior laryngeal nerve. However, this was not possible in all cases either because of damage to the nerve (indicated by an absence of antidromic field potentials), or when the nerve on only one side had been dissected while recordings were made from the contralateral side. These antidromic field potentials could be recorded on the left side in 14 of 17 experiments in which the superior laryngeal nerve was dissected only on one side. In the remaining experiments in which both nerves were dissected, field potentials were recorded on both sides in 4 animals, and only on one side in 5.

In some experiments (n = 6) a limited extracellular mapping of *inspiratory* units was performed from the level of the obex (calamus scriptorius) to 1.0 mm rostral (rostral VRG), guided by antidromic field potentials evoked by stimulation of the cervical portion of the vagus nerve. Following the initial tracking with extracellular microelectrodes, intracellular recordings were made with bevelled glass microelectrodes containing 2% biocytin (Horikawa and Armstrong, '88) in 0.3 M KCl (resistance, 60–100 MΩ). Tracking was done with electrodes oriented approximately vertically to the dorsal medullary surface. Only neurons which had a membrane potential, measured during the phase of maximal hyperpolarization, greater than −30 mV for a period of more than a few minutes, were considered for further analysis. This cutoff level of membrane potential was chosen on the basis of our observation that impalements with less negative potentials were generally unstable (the potential gradually deteriorating) while impalements with a potential greater than −30 mV were generally more stable and showed action potentials. Biocytin was injected intracellularly by using depolarizing current pulses (400 ms, 2–8 nA) at 2 Hz, for up to 20 minutes. The range of charge transfer was 4.5 to 70 nA × min.

All recorded signals were monitored on a multi-channel pen recorder, and selected signals recorded on a thermal array recorder (Nihon Kohden, RTA 1100 M) or stored on digital tape (Vetter, Model 3000) for subsequent off-line analysis.

Histological analysis

At least 1.5 hours after the last intracellular injection, rats were perfused transcardially with 0.9% NaCl containing 10 mM sodium nitrite and 1,000 u/liter heparin, followed by approximately 500 ml of 0.1 M phosphate buffer (pH 7.4) containing 4% formaldehyde and 0.2% picric acid. The brainstem was then removed and stored overnight in the same fixative at room temperature. Parasagittal sections (33 μm) of the medulla oblongata were cut with a Vibratome. The free-floating sections were rinsed in 0.1 M phosphate-buffered saline (PBS) and incubated for 4 hours with Streptavidin-Texas red (Sigma) diluted 1:200 in buffer containing Triton X-100 0.3% (v/v), and (in mM): NaCl 120, KCl 5, NaH_2PO_4 1.5, Na_2HPO_4 8.5, Tris base 10, sodium merthiolate 1, pH 7.4. All incubations were conducted at room temperature with continuous agitation.

Histological analysis was carried out in several stages. First, sections were mounted serially on plain glass slides and coverslipped with 0.1 M PBS. Sections containing Texas red-labeled neurons and their processes were selected with the aid of a fluorescence microscope. Second, the selected sections were removed from slides, rinsed in 0.1 M PBS and incubated for 4–12 hours in DAPA-biotin-HRP (Sigma) diluted to 100 mg protein/ml. After three 10 minute washes in 0.1 M PBS, sections were incubated for 15–20 minutes in 50 mM Tris-HCl buffer (pH 7.6) containing diaminobenzidine (0.02%), nickel ammonium sulfate (0.6%), and hydrogen peroxide (0.003%). Sections were mounted serially onto gelatin-coated slides, dehydrated and coverslipped. The permanently stained cells (hard copies) were used for standard camera lucida reconstructions as well as bouton counts (e.g., Otake et al., '90), which were made with 25× or 40× microscope objectives. For measurements of the size of the cell bodies (in the parasagittal plane), the mean values were taken of the major and minor axes of the best-fit ellipse.

Sixty-three or 100× oil immersion objectives were used to examine fine processes and possible appositions between presynaptic bouton-like profiles belonging to labeled BOT neurons and the dendrites of inspiratory neurons injected in the rostral VRG. Two adjacent neuronal profiles (e.g., a bouton and a dendrite) were said to be in close apposition if they were apposed side by side and there was no discernible space between them (cf. Pilowsky et al., '92).

Finally, the coverslips were removed and the sections were counterstained with a standard Nissl technique. Although this step decreased the intensity of staining of the cell bodies and processes belonging to injected neurons, it allowed them to be located with respect to major nuclei in the ventral part of the medulla oblongata. No correction was made for tissue shrinkage in morphometric measurements. Shrinkage, mainly due to tissue dehydration, is known to be of the order of a few (2–6) percent (e.g., Cameron et al., '85). However, there appears to be no clear relationship between the degree of shrinkage and the degree to which the size of intracellularly labeled cells change (cf. Grace and Llinás, '85).

RESULTS

General properties of expiratory neurons in the rostral ventrolateral medulla (RVLM)

Recordings were made in the RVLM, in the region between 1.0 and 2.5 mm rostral to the obex, 1.2 and 2.5 mm lateral to the midline, and 2.0 to 3.6 mm below the dorsal medullary surface. The extent of the tracking in the rostrocaudal and mediolateral directions was chosen to cover the area containing the rostral column of expiratory neurons as defined in the extracellular study of Ezure et al. ('88). One hundred and forty-nine neurons were impaled (membrane potential 45.4 ± 9.5 mV, mean ± S.D.; all but seven between 1.2 and 2.4 mm rostral to the obex) which exhibited depolarizing shifts of the membrane potential during expiration, often associated with firing. Hyperpolarizing shifts of membrane potential during inspiration could be reversed following injection of chloride ions in many cases (not illustrated). Figure 1 shows the location of all impaled expiratory cells. A relatively large mediolateral (Fig. 1A) and dorsoventral (Fig. 1B) scatter of recording positions resulted from plotting data from all animals together, using the obex (calamus scriptorius) as a reference point. In individual animals, the maximum mediolateral distance between recorded neurons had a range of 0.1 to 0.9 mm (mean, 0.48 mm), and the maximum dorsoventral distance a range of 0.1 to 1.1 mm (mean, 0.63 mm)

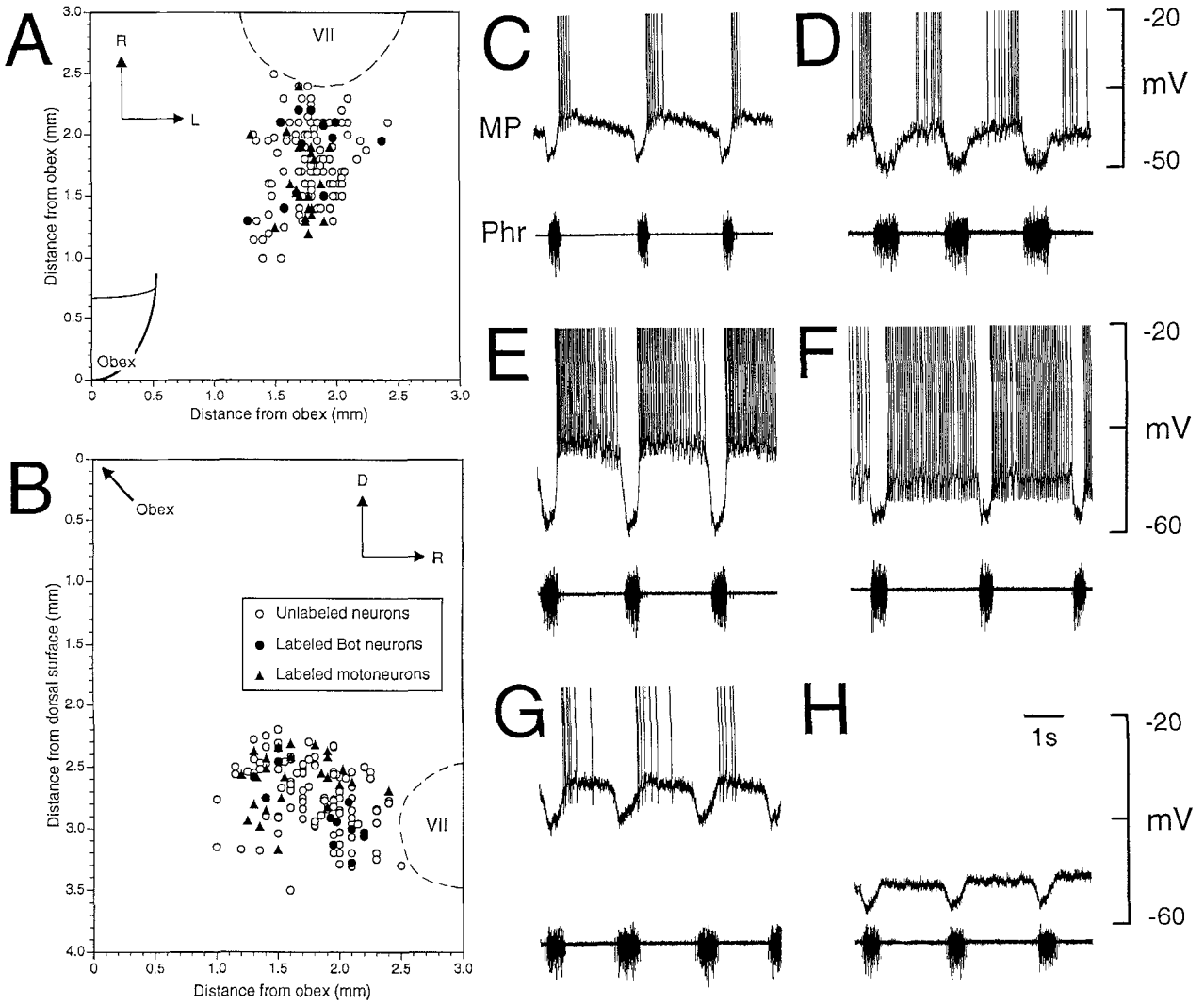

Fig. 1. Distribution (A,B) and examples of membrane potentials and discharge patterns (C–H) of expiratory neurons impaled in the region of the BOT. **A,B:** Dorsal view and lateral projection of medulla oblongata, showing location of neurons based on stereotaxic coordinates (data from 26 animals). Position of the facial nucleus drawn from one rat. Compact and semicompact formations not shown due to variations in dorsoventral and mediolateral positions observed between animals. **C–H: Upper traces,** membrane potential (MP); **lower traces,** activity of the phrenic nerve (Phr). C, E: E-DEC (decrementing expiratory) neurons. D: E-AUG (augmenting expiratory) neuron. F: E-CON (constant expiratory) neuron. G,H: E-DEC neuron initially showing a decrementing pattern of spiking (G) which changed to a constant pattern of membrane potential (H). In C–G, spikes truncated at approximately −20 mV. D, dorsal; L, lateral; R, rostral; VII, facial nucleus.

suggesting less variability in cell column boundaries than shown in Figure 1.

All expiratory neurons were classified into three types: augmenting expiratory (E-AUG), constant expiratory (E-CON), and decrementing expiratory (E-DEC). Examples of these patterns are shown in Figure 1C–H. E-AUG neurons (n = 10) showed an augmenting pattern of firing and membrane depolarization (or of membrane depolarization alone) during expiration. E-CON neurons (n = 67) showed an approximately constant (plateau) level of firing or membrane potential. E-DEC neurons (n = 72) either had a clear decrementing pattern of firing or, if spike inactivation had occurred, of membrane potential. However, a few E-DEC neurons showed a decrementing pattern of firing before spike inactivation, but a constant level of depolarization after inactivation (Fig. 1G,H).

As postinspiratory activity (Richter and Ballantyne, '88) was not usually found in recordings from the phrenic nerve in our vagotomised animals (Figs. 1C–H; 2C,D; 3C,F; 4B; 5A; 7B; 8), it was not possible to distinguish a group of neurons active in postinspiration, referred to in other studies as postinspiratory (e.g., Schwarzacher et al., '91; Zheng et al., '91b). For this reason, neurons showing a decrementing pattern of activity (or membrane depolarization) during expiration were referred to as E-DEC (see also Manabe and Ezure, '88; Ezure et al., '88). This was also the case for a few neurons which showed only a short period of spiking during the early stage of expiration (e.g., Fig. 1C).

Morphology

Of 149 expiratory neurons, 41 were labeled intracellularly and a hard copy recovered under bright field micros-

TABLE 1. Classification of Labeled Expiratory Neurons

Type	n	E-AUG	E-DEC	E-CON
Nonbulbospinal BOT neurons	9 (22%)	2	3	4
Bulbospinal BOT neurons	3 (7%)	1 (11.7 m/s[1])	0	2 (9.5 m/s and 4.9 m/s[1])
Motoneurons	29 (71%)	1	14	14
Total	41 (100%)	4	17	20

[1]Calculated conduction velocities.

copy (Table 1). In each case, the soma was dark and homogenously stained, and details of dendritic morphology were clearly visible throughout the whole extent of the dendritic tree. Axons were darkly stained up to 4.5 mm from the cell body (range, 2.7–4.5 mm), and could often be traced to the rostral or caudal edge of the section (Figs. 3A; 5A; 7A). In three expiratory interneurons (see below), an axon could be traced to the contralateral side. However, the longest contralateral projection identified was of an inspiratory neuron labeled in the rostral VRG (Fig. 8, neuron 1). The axon could be traced for more than 3 mm from the point at which it crossed the midline (not illustrated). Fine axon collaterals showed generally well-stained bouton-like structures (e.g., Fig. 5C–E), which could easily be counted (histograms, Figs. 3–8). Fine details could be also observed in distal parts of dendritic trees. Some distal dendrites had a beaded appearance resembling en passant boutons of axon collaterals (e.g., Fig. 2G).

Motoneurons. Twenty-nine impaled and labeled cells showed morphological features characteristic of motoneurons (Fig. 2A,B,E,F). They had relatively large, multipolar somata (average diameter, 29.7 ± 6.1 μm), which issued 5 to 7 dendritic trunks. Dendrites, which were up to 700 μm in length, projected in all directions with a relative paucity of projections in the dorsal direction. In some cases, the projections had a caudomedial and rostrolateral prevalence (Fig. 2A). Axons, after leaving the somata, coursed dorsomedially, then turned sharply at various distances from the cell body to travel ventrolaterally. This type of axon trajectory is characteristic of motoneurons of the nucleus ambiguus (e.g., Kalia and Mesulam, '80). No axon collaterals were found.

Interneurons. Twelve neurons were recovered that were classified as interneurons on the basis of morphological criteria and, in three cases, antidromic response from the spinal cord. These neurons generally had a lower membrane potential (mean for group, −44 ± 6 mV; E-AUG, 47 ± 9 mV, n = 3; E-DEC, 43 ± 5 mV, n = 3; E-CON, 42 ± 4 mV, n = 6; no significant difference among means) than motoneurons (−48 ± 8 mV, n = 29). Some (e.g., Figs. 3F and 4B) displayed large afterhyperpolarizations, which was also the case in most of the recordings from motoneurons (e.g., Fig. 2D). Therefore, a distinction between interneurons and motoneurons could not be made on the basis of the amplitude of afterhyperpolarizations as suggested by Zheng et al. ('91b). Axons branched within the medulla and issued many collaterals with frequent varicosities suggestive of presynaptic boutons. Cell somata were small (average diameter, 19.6 ± 5.4 μm compared with 29.7 ± 6.1 μm for motoneurons, significant difference, t-test, $P < .01$), and oval or fusiform in shape. The somata of nine of these neurons were located ventral or ventromedial to the compact and semicompact formations (Figs. 3A,D; 4A,B; 7, neuron 2; 8, neuron 2), and the remaining three just caudal to the compact/semicompact formation (Fig. 5A). Interneurons generally had fewer primary dendrites (range, 2–5) than motoneurons (range, 5–7), and demonstrated a lesser degree of branching (range for interneurons, 2–4 branch points; motoneurons, 4–6 branch points).

E-AUG neurons. Three of twelve labeled interneurons showed an E-AUG pattern of activity. One E-AUG neuron could be antidromically activated from the ipsilateral side of the spinal cord (not illustrated), one did not respond to antidromic stimulation (Fig. 3D–F), and one could not be tested for spinal projections due to spike inactivation (Fig. 3A–C). Cell somata (average diameter, 17.4 ± 5.2 μm, mean ± S.D.) were located ventral to the compact and semicompact formations of the nucleus ambiguus, 200 to 350 μm from the ventral border of the compact formation. Two E-AUG cells issued three primary dendrites each. In each case, two of the three dendrites extended ventrally and one dorsally (Fig. 3A). The other E-AUG cell had four primary dendrites which had branches extending in all directions (Fig. 3D). Dendrites of all these neurons were approximately 500 μm long.

Originating from the cell body or a proximal dendrite (e.g., Fig. 3B), the axons of all three cells coursed dorsomedially, and then bifurcated into branches which projected caudally (descending axon) and dorsomedially towards the midline. No collaterals were observed arising from the dorsomedial branches. The descending axons immediately issued collaterals that distributed boutons in the area of the cell body and in the region immediately rostral. As the descending axons progressed caudally, they issued more collaterals which travelled mainly ventrally and distributed boutons to the areas of the BOT and of the rostral and caudal parts of the VRG.

E-DEC neurons. None of three E-DEC interneurons recovered could be antidromically activated from the spinal cord. Two (shown in Fig. 4A and B) were located ventral to the compact formation (350 and 40 μm from its ventral border, respectively), and the third (not illustrated) was more caudal, ventral to the caudal portion of the semicompact formation. Average diameters of the somata were 15.6 ± 4.0 μm (mean ± S.D.). All three cells had three primary dendrites (Fig. 4A,B), one dorsal, one ventral, and one rostral. In the neuron shown in Figure 4B, the rostral dendrite soon turned dorsally. These dendrites were up to 600 μm long.

After leaving the cell body or a main dendrite, axons travelled dorsally 100 to 300 μm, then turned sharply to run in a ventral direction. The descending axon issued several collaterals, then turned again, going caudally and ramifying into three branches. One of these coursed dorsomedially and two caudally. In one case (Fig. 4B), the dorsomedial branch turned caudal and soon terminated, and there was an additional rostral branch. All branches issued collaterals with boutons. The latter were most numerous in two areas: ventral to the compact and semicompact formations, and caudal to this, in the region of the rostral VRG. Fewer boutons were observed in the region of the caudal VRG.

E-CON neurons. Six of the twelve labeled interneurons belonged to this category. Two could be antidromically activated from the contralateral spinal cord (one antidromically activated neuron is shown in Fig. 7A, neuron 2, and two nonantidromically activated neurons in Figs. 5A and 8, neuron 2). Cell bodies of four neurons were located ventromedial to the compact and semicompact formations (up to 200 μm from the border of the compact formation), and two

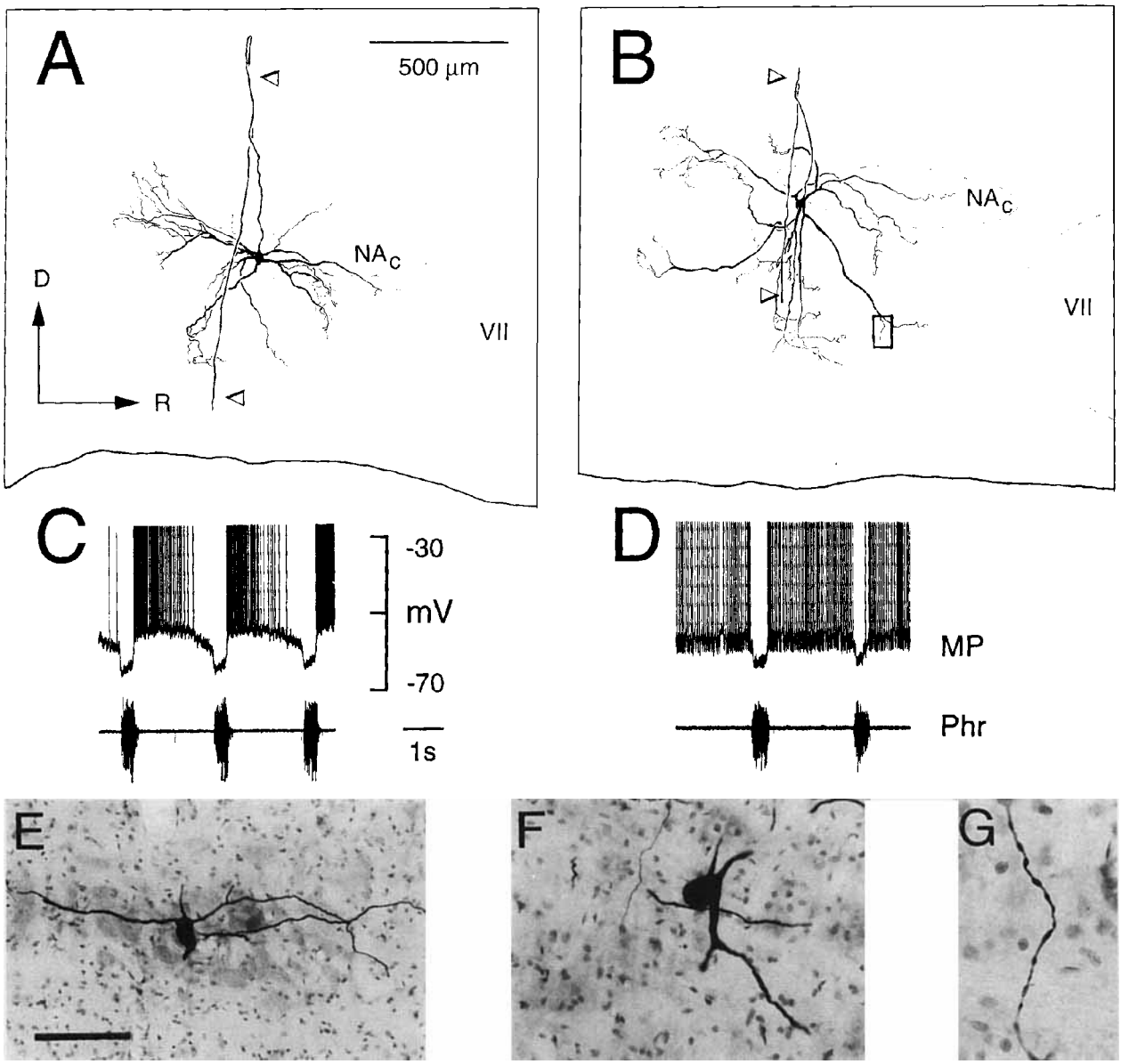

Fig. 2. Features of two expiratory motoneurons labeled in the rostral part of the nucleus ambiguus. **A:** E-DEC motoneuron reconstructed from 11 parasagittal 33 μm sections. **B:** E-CON motoneuron reconstructed from 34 sections. Open triangles indicate axons. **C,D:** Intracellular recordings from neurons shown in A and B, respectively. **Upper traces:** membrane potential (MP); **lower traces,** activity of the phrenic nerve (Phr). **E:** Photomicrograph of section containing cell body of motoneuron shown in A, counterstained with cresyl violet. Note cell bodies of adjacent neurons in the compact formation of the nucleus ambiguus. **F:** Photomicrograph of cell body of motoneuron shown in B. **G:** A dendrite of the neuron reconstructed in B (boxed area in B) showing swellings reminiscent of en passant boutons of axon collaterals. NA_c, compact and semicompact formations of nucleus ambiguus. Other abbreviations as in Figure 1. Scale bar in E = 130 μm for E, 80 μm for F, and 40 μm for G.

just caudal to the compact formation (Fig. 5A). E-CON cells had an average soma size of 22.9 ± 4.8 μm (mean ± S.D.) and two to five primary dendrites, which extended up to 600 μm from the cell body and projected either dorsoventrally like those of E-DEC and E-AUG neurons (Fig. 8, neuron 2), or in all directions (Figs. 5A; 7A, neuron 2).

Five E-CON neurons demonstrated similar axonal morphology to that of E-AUG and E-DEC neurons. Their axons coursed dorsally then branched into a dorsomedial, and one or two caudal branches (Figs. 7A, neuron 2; 8, neuron 2), although in one case (not illustrated) the dorsomedial projection was limited, like that of the E-DEC neuron shown in Figure 4B. The axon of the bulbospinal neuron shown in Figure 7A was somewhat atypical; its dorsomedial branch first coursed rostrally and medially, issuing several collaterals, before returning to pass the soma and running dorsomedially to project to the contralateral side. Also, one cell (not illustrated) had a dorsomedial branch that turned caudally about 1,300 μm dorsal to the cell body, and another (Fig. 8, neuron 2) had a collateral that ran rostrally

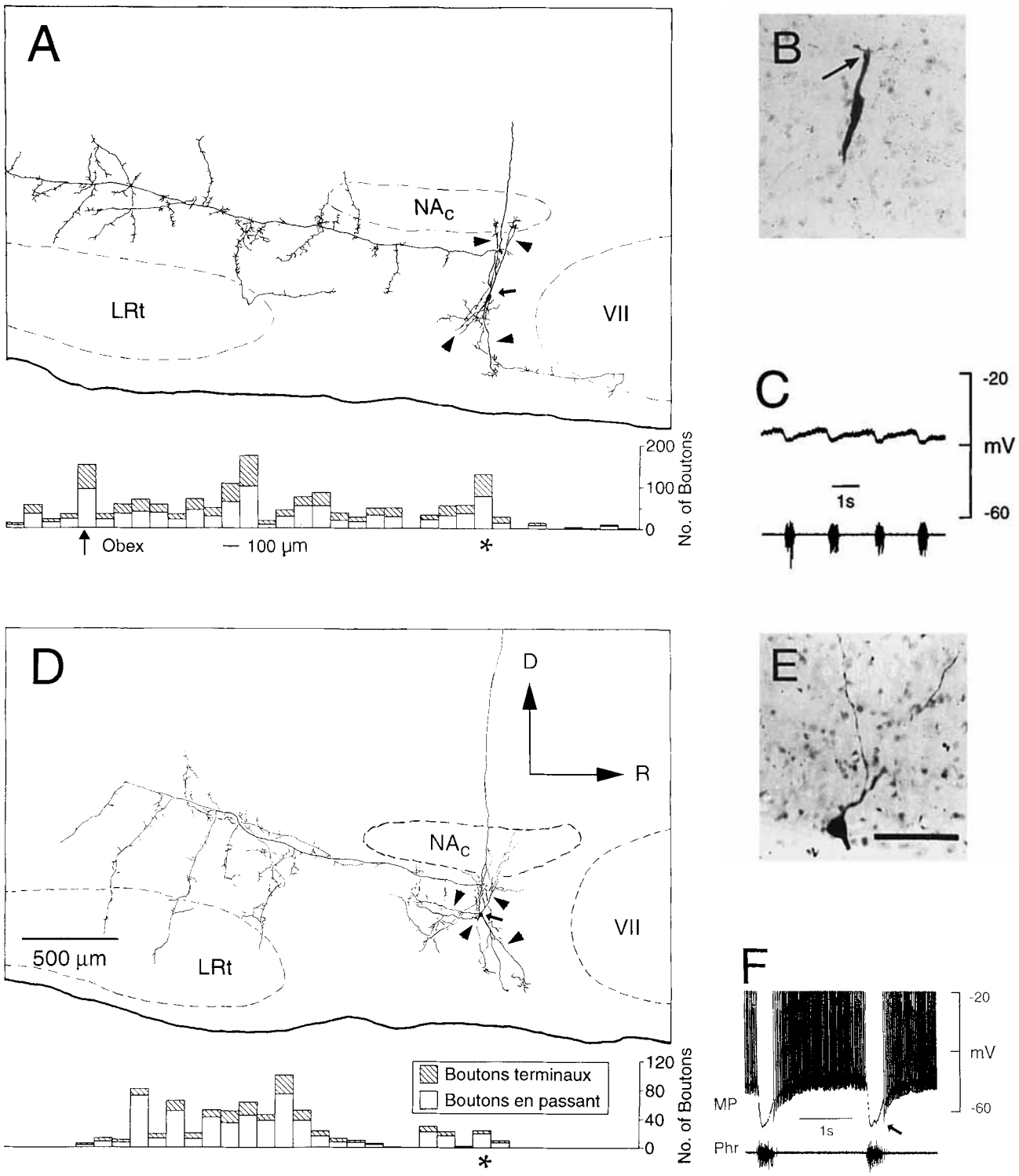

Fig. 3. Morphology and electrophysiology of two E-AUG BOT neurons. **A,D:** Camera lucida reconstructions made from 13 and 22 parasagittal sections, respectively. Arrowheads indicate dendrites; arrows show the position of the cell bodies. Histograms below each reconstruction show distribution of bouton-like structures counted in 100 µm wide sequential rostrocaudal segments. Asterisks indicate cell bodies and arrow the level of obex. **B,E:** Photomicrographs of cell bodies of neurons shown in A and D, respectively. Arrow in B shows the dendritic origin of the axon. **C,F:** Intracellular recordings from the neurons shown in A and D, respectively (upper traces, membrane potential, MP; lower traces, activity of the phrenic nerve, Phr). In F, arrow indicates large afterhyperpolarization, spikes truncated at −20 mV. D; dorsal; R, rostral; LRt, lateral reticular nucleus; NA_c compact and semicompact formations of nucleus ambiguus; VII, facial nucleus. Scale bar in E = 80 µm for B and E.

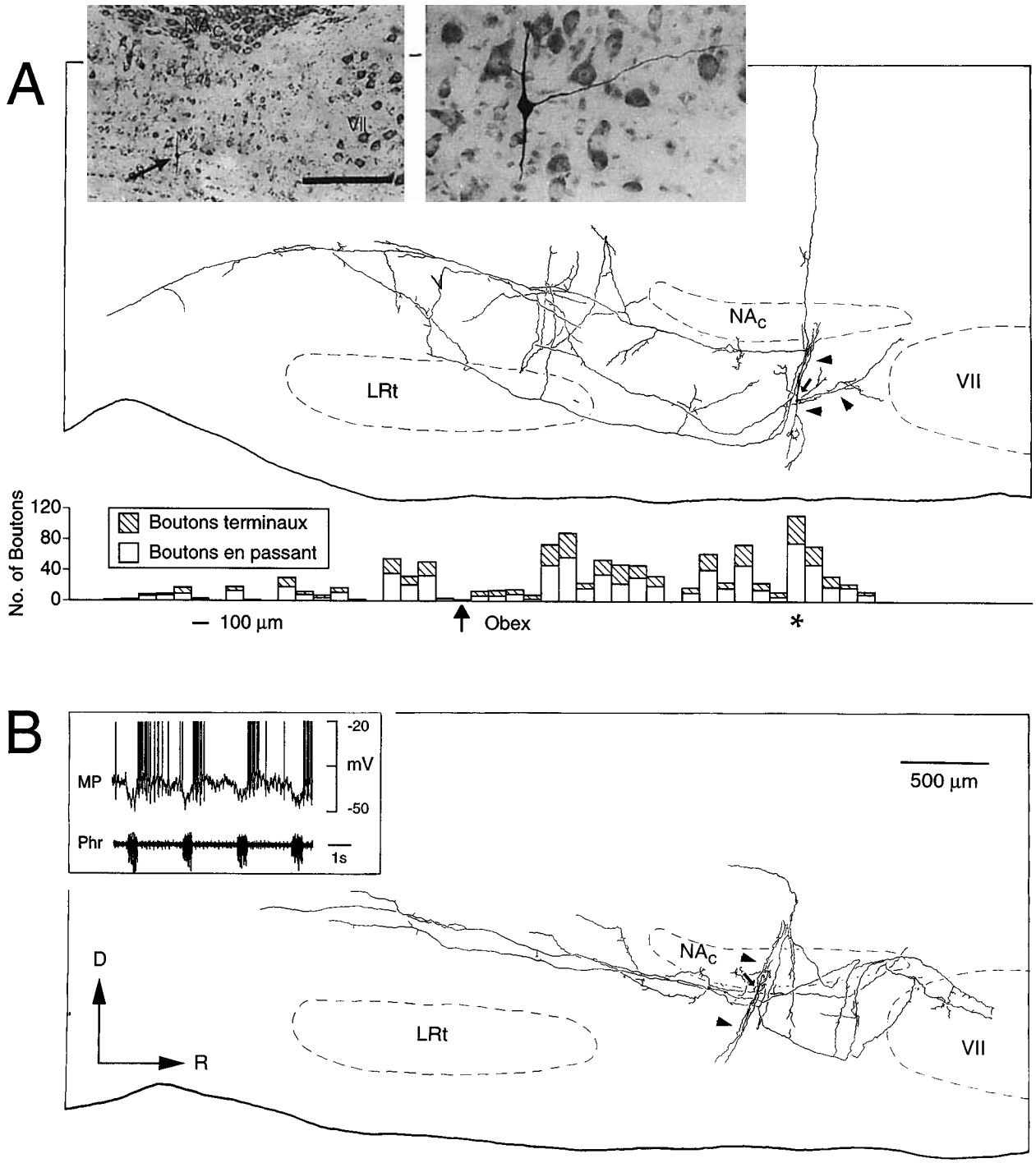

Fig. 4. Data from two E-DEC neurons. **A:** Camera lucida reconstruction from 40 parasagittal sections and histogram showing bouton distribution (see legend to Fig. 3). **Insets** show low and high power photomicrographs of the section containing the cell body (cell body indicated by arrow in left inset) counterstained with cresyl violet. Note in left inset the compact and semicompact formations (NA_c) and facial nucleus (VII). **B:** Reconstruction from 51 parasagittal sections. **Inset:** Intracellular recording showing membrane potential (MP) and phrenic nerve activity (Phr). In A and B, arrowheads indicate dendrites, arrows show the cell bodies. Abbreviations as in Figure 3. Scale bar in left inset in A = 300 μm for left inset, 100 μm for right inset.

from the dorsomedial branch in the dorsal medulla. All five cells issued collaterals distributing boutons rostral and caudal to the cell soma.

One E-CON cell, shown in Figure 5, had a different type of axonal morphology from the five so far described. Arising from the soma, the axon coursed dorsomedially, then bifurcated twice. One branch continued dorsomedially towards the hypoglossal nucleus where it issued collaterals (Fig. 5E), and then turned sharply ventromedial, descending until it again reached the level of the cell body, where it

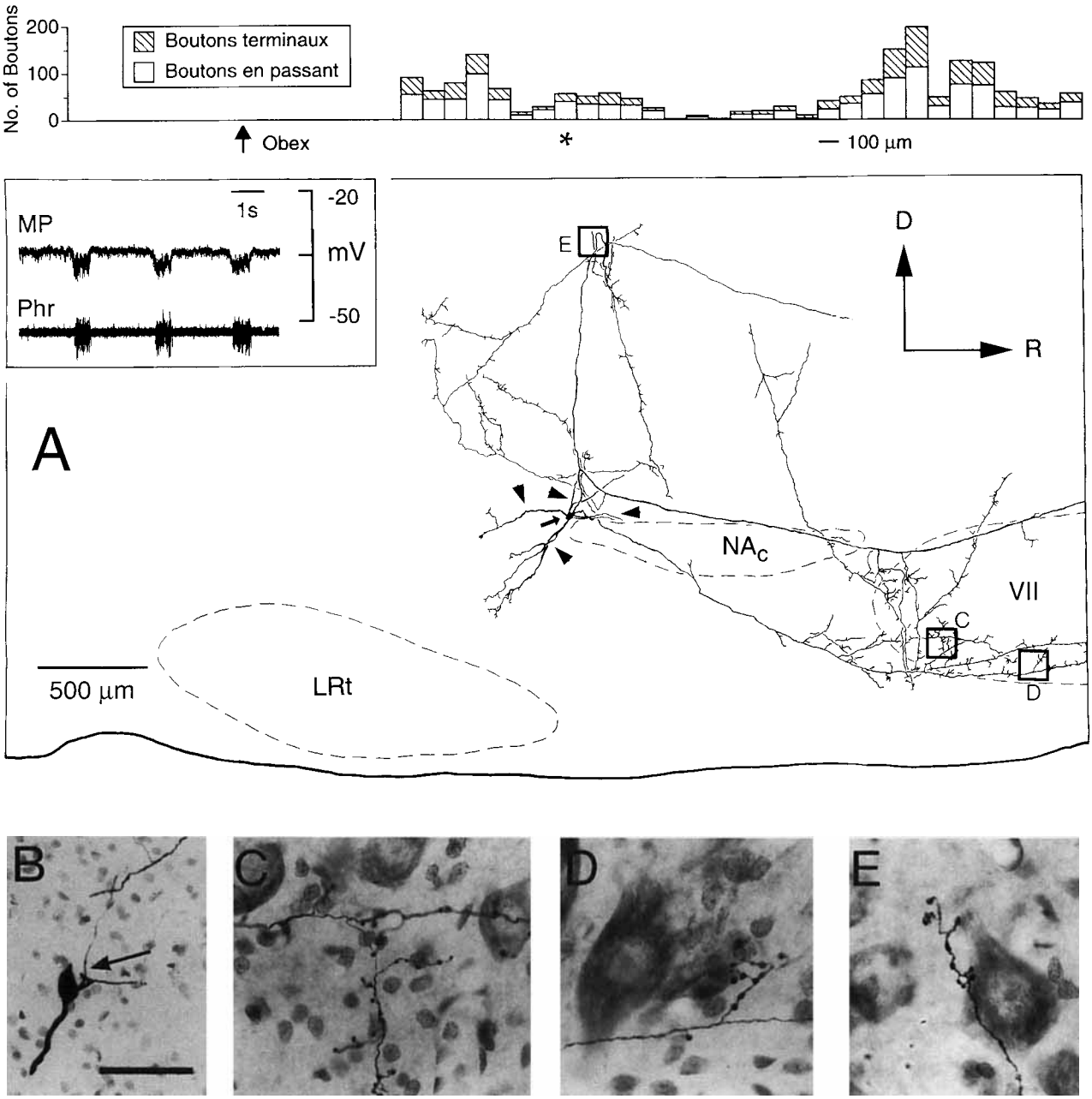

Fig. 5. E-CON neuron showing rostrally projecting axonal branches. **A:** Camera lucida reconstruction from 60 parasagittal sections. Arrowheads indicate dendrites, arrow shows the cell body. Small boxes indicate position of photomicrographs (C,D, and E). **Inset:** Membrane potential (MP) and phrenic nerve activity (Phr). Histogram shows bouton distribution (see legend to Fig. 3). **B:** Photomicrograph of cell body. Origin of the axon is indicated by an arrow. **C,D:** Photomicrographs of axon collaterals and boutons near the ventral border of the facial nucleus corresponding to the boxes in A. **E:** Axon collateral and boutons in the region of the hypoglossal nucleus (box in A). Abbreviations as in Figure 3. Scale bar in B = 80 μm for B, 40 μm for C, 30 μm for D and E.

crossed the midline. The remaining two branches travelled rostrolaterally, passing along the dorsal and ventral borders of the facial nucleus, and issued collaterals which entered this nucleus or ran near its border (Fig. 5C,D). The branch travelling along the dorsal borders of the facial nucleus continued rostrally to the pons.

Synaptic targets of BOT neurons

The bouton-like structures of all labeled interneurons, with the exception of one E-CON neuron shown in Figure 5, were distributed within a well defined area which includes the regions of the BOT and the VRG (Figs. 3, 4, 7, and 8). The ratio of boutons en passant to boutons terminaux appeared to be similar in all three neuron types. This ratio in all cells examined (2 E-AUG, 2 E-DEC, and 4 E-CON) was 1.95 ± 0.56 (mean ± S.D.). The cumulative graph of boutons of these eight interneurons (Fig. 6) shows the largest number of boutons near the parent cell bodies, 1,800–1,900 μm rostral to the obex, mainly at the level of the caudal half of the compact formation. A second peak

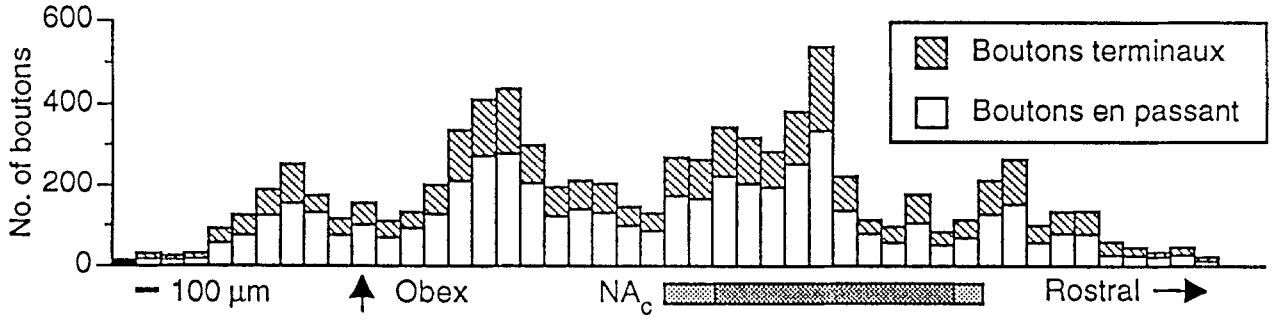

Fig. 6. Histogram showing the rostrocaudal distribution of boutons counted in 8 BOT expiratory neurons (2 E-AUG, 2 E-DEC, and 4 E-CON). Dark bar shows position of the compact and semicompact formations of nucleus ambiguus (NA_c); lighter bars at either end show variation in their length among animals.

was in the region of the rostral VRG, 600–700 µm rostral to obex. A lesser, although still significant, concentration of boutons was observed in the region of the caudal VRG, reaching a maximum about 300–400 µm caudal to obex. A fourth peak, which could be observed rostral to the BOT, resulted mainly from boutons of the E-CON cell shown in Figure 5.

Inspiratory neurons of the rostral VRG were selected for examination as possible synaptic targets of ipsilateral BOT neurons, as evidence exists that these neurons are inhibited by BOT expiratory neurons in the cat (e.g., Jiang and Lipski, '90), and a large number of bouton-like structures were observed in the rostral VRG region in our study. Recordings from these cells were made between the level of the obex and 1.0 mm rostral, from 1.0 to 1.8 mm lateral to the midline, and from 2.0 to 3.2 mm below the dorsal medullary surface. All inspiratory neurons labeled intracellularly with biocytin (n = 5) were located between 0.5 and 0.9 mm rostral to obex, generally coinciding with the peak in the bouton distribution at this level (Fig. 6).

Five pairs consisting of one BOT expiratory interneuron and one inspiratory cell in the rostral VRG were recovered and examined with light microscopy. The characteristics of the BOT neurons have been described above. Two pairs consisted of an inspiratory motoneuron (identified by morphological criteria described for expiratory motoneurons; see Results: Motoneurons) and an expiratory interneuron (E-DEC and E-CON). These two pairs are not illustrated because the axons of the two BOT neurons did not project near the motoneurons (see below). One pair comprised an inspiratory bulbospinal neuron and an E-CON neuron, and is shown in Figure 7. Finally, two pairs consisted of an inspiratory nonbulbospinal interneuron and an E-CON interneuron (one pair is shown in Figure 8). All five inspiratory cells were well stained and details of dendritic morphology were clear. In all cases, except for the two pairs mentioned above, the collaterals and boutons of BOT neurons could be observed in proximity to the dendrites of inspiratory neurons. However, in none of these cases could close appositions between axon varicosities of expiratory neurons and dendrites or somata of inspiratory neurons be found. Axonal branches often crossed dendrites in the same section, but examination using ×63 or ×100 oil immersion objectives indicated that there was always a gap between the varicosities and the dendrite of the inspiratory neuron. Thus, close appositions (as defined in Methods) between axons and dendrites were not present.

DISCUSSION

Although in four previous studies, conducted in adult rats, intracellular recordings were made from respiratory neurons located near the rostral end of the VRG (Pilowsky et al., '90; Zheng et al., '91a,b, '92), to our knowledge this is the first detailed morphological study of expiratory neurons in this region. In the study conducted in our laboratory by Pilowsky et al. ('90), recordings were made from nine expiratory neurons, but axonal projections were described only for two neurons, which were reconstructed from coronal sections after intracellular labeling with Lucifer yellow. One of the two cells was an interneuron with axon collaterals near the rostral end of the nucleus ambiguus, while the second was a motoneuron. In the study by Zheng et al. ('91b), three E-DEC neurons (called "postinspiratory" by the authors) were injected with horseradish peroxidase more than 1.0 mm rostral to the obex. All three turned out to be motoneurons. Before discussion of the properties of neurons labeled in the present study, comment will be made on the terminology used to describe respiratory neurons in this medullary region.

Terminology

There has been inconsistency in the literature regarding the nomenclature of respiratory neurons located in the RVLM. The term Bötzinger Complex was first used by Lipski and Merrill ('80) to name a concentration of expiratory neurons projecting to the contralateral nucleus of the solitary tract in the cat. Other axonal projections of this group of inhibitory interneurons were described in subsequent studies, including projections to other respiratory parts of the medulla oblongata and spinal cord (Fedorko and Lipski, '81; Bianchi and Barillot, '82; Merrill et al., '83; Fedorko and Merrill, '84; Otake et al., '88; Jiang and Lipski, '90: see also Kalia et al., '79; Smith et al., '89). Although the term Bötzinger Complex (BOT) was used in many of these and in other studies (see Introduction), some authors used the terms "retrofacial group," "retrofacial respiratory (expiratory) neurons," or "respiratory neurons in the region of the retrofacial nucleus" to emphasise the close anatomical association of these neurons with the retrofacial nucleus (e.g., Bianchi and Barillot, '82; Grélot and Bianchi, '87; Shannon and Lindsey, '87). Still others have used the term 'rostral medullary respiratory (expiratory) neurons' to stress the fact that this neuronal group is located near the

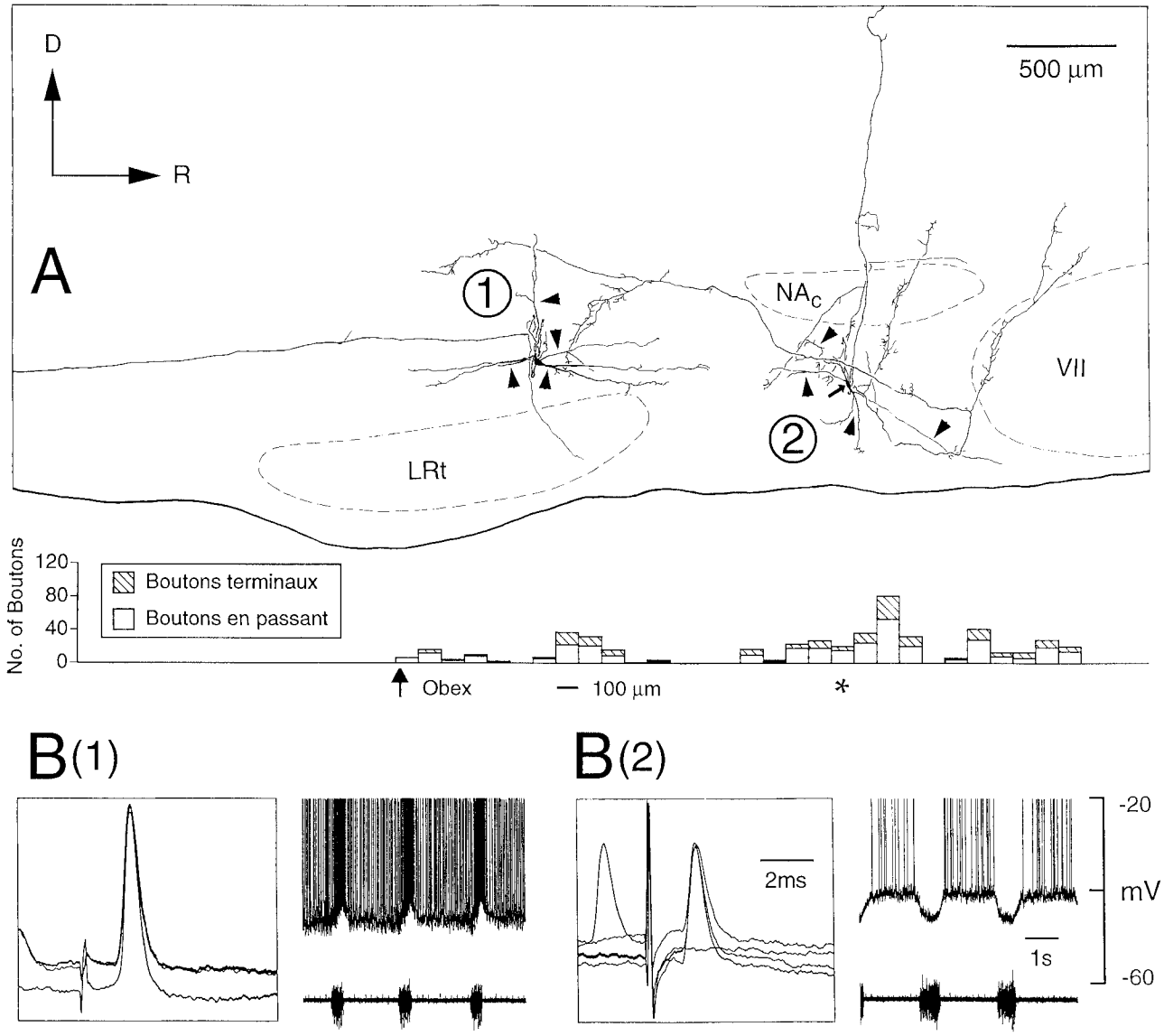

Fig. 7. Features of a pair of neurons labeled to examine possible synaptic contacts. **A:** Camera lucida reconstruction from 58 parasagittal sections. Neuron 1 was a bulbospinal augmenting inspiratory neuron, neuron 2 a bulbospinal BOT E-CON neuron. Arrowheads indicate dendrites of both neurons and the arrow, the cell body of the BOT neuron. Histogram shows rostrocaudal distribution of boutons of neuron 2 (see legend to Fig. 3). **B:** Intracellular recordings from neuron 1 [B(1)] and neuron 2 [B(2)] showing (left) antidromic spikes evoked by stimulation at the junction between the C2 and C3 segments of the spinal cord (3 and 4 superimposed sweeps, respectively). Antidromic activation from the spinal cord of neuron 1 was ipsilateral, and that of neuron 2 was contralateral. Note in B(2) the collision between the antidromic spike and a spontaneous spike occurring just before the stimulus. On the right, patterns of membrane potential. **Upper traces,** membrane potential; **lower traces,** phrenic nerve activity. Abbreviations as in Figure 3.

ponto-medullary junction (e.g., Bianchi et al., '88; Grélot et al., '88).

We use the term Bötzinger Complex to refer to a concentration of propriobulbar and bulbospinal respiratory (mainly expiratory) neurons located in the rostral part of the medulla oblongata, mainly ventral and ventromedial to the rostral divisions of the nucleus ambiguus. Although inspiratory interneurons in this medullary region can be regarded as part of the BOT (Bianchi et al., '88; Otake et al., '90; Anders et al., '91), motoneurons are not (see below). It should be emphasised that, although BOT neurons have a well defined anatomical location, they do not form a distinct cytoarchitectonic nucleus. Therefore, "Bötzinger Complex" is a functional rather than an anatomical term.

Motoneurons

Although the main aim of this study was to characterise BOT neurons (i.e., interneurons), mention must be made of the relationship between these neurons and respiratory (expiratory) motoneurons found in the rostral part of the nucleus ambiguus. Motoneurons were, in fact, the most commonly impaled and labeled cells in our study. However, none of them could be classified as a motoneuron on the

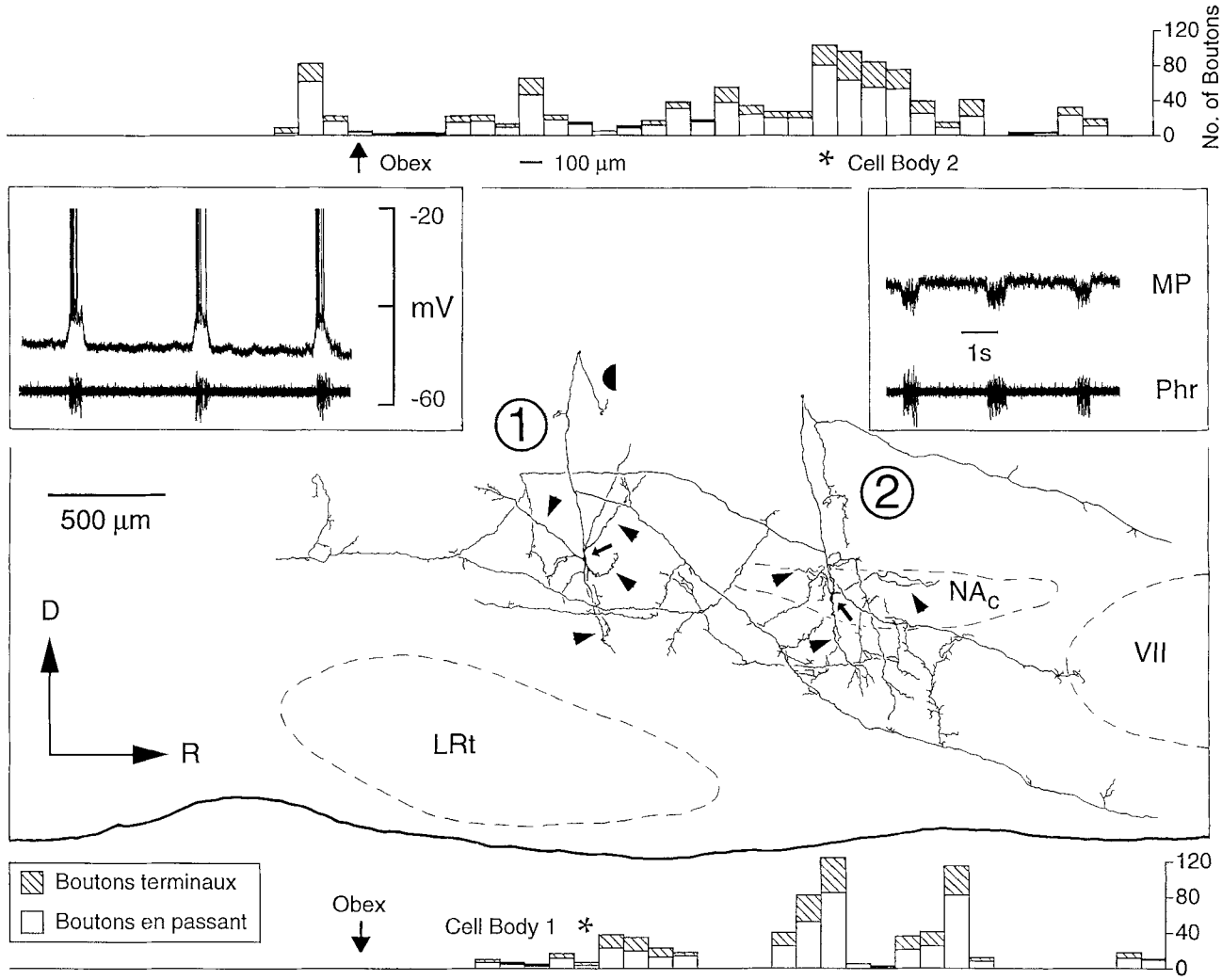

Fig. 8. Data from another pair of neurons labeled to examine possible synaptic contacts. Camera lucida reconstruction of two neurons from 60 parasagittal sections. Neuron 1 was a decrementing inspiratory interneuron located in the rostral VRG, and neuron 2 was a BOT E-CON cell. Arrowheads indicate dendrites, and arrows show the cell bodies of both neurons. Semicircle indicates axon collateral traced contralaterally. Note that the axons of both neurons have collaterals. No close appositions between axon terminals and dendrites were seen. **Insets** show intracellular recordings from the two neurons: **left,** a recording from neuron 1; **right,** recording from neuron 2 (upper traces, membrane potential, MP; lower traces, phrenic nerve activity, Phr). Upper histogram shows rostrocaudal distribution of boutons of neuron 2. Lower histogram shows distribution of ipsilateral boutons of neuron 1. Abbreviations as in Figure 3.

basis of their antidromic response to stimulation of the cervical portion of the vagus or the superior laryngeal nerves (Zheng et al., '91b). (In fact, no attempts were made to label neurons in the BOT region that could be antidromically activated from these nerves, as they were obviously motoneurons.) Therefore, it is likely that the axons of labeled motoneurons projected in *pharyngeal* branches of the vagus nerve, which are not easily accessible and therefore were not stimulated in the present study (see Grélot et al., '89; Zheng et al., '91b). These neurons were recognised as motoneurons on the basis of the large size of their cell bodies, the typical axonal trajectories, and the lack of axon collaterals (cf. Zheng et al., '91b).

In a number of previous electrophysiological studies of this area in both cats and rats (Pantaleo and Corda, '85; Orem and Brooks, '86; Shannon and Lindsey, '87; Bianchi et al., '88; Bongianni et al., '88; Ezure et al., '88; Speck, '89; Li et al., '91), no distinction was made between respiratory interneurons and motoneurons, and the somewhat imprecise term Bötzinger (or retrofacial, or rostral) *region* was used. In a recent study by Zheng et al. ('91b), almost all decrementing expiratory neurons (referred to as postinspiratory), which were intracellularly labeled in this medullary area, turned out to be motoneurons rather than true BOT neurons. Clearly the distinction between BOT neurons and motoneurons is important to differentiate the function of these neuronal groups. It may be noted that an analogous distinction has been proposed between interneurons and motoneurons in the VRG (Kalia, '81). In the caudal and middle parts of the medulla, respiratory neurons of the VRG in the retroambiguus and para-ambiguus nuclei are functionally distinct from laryngeal motoneurons of the nucleus ambiguus, although they occupy a similar region (see also Núñez-Abades et al., '91).

BOT neurons

A relatively low number of stable intracellular recordings from BOT neurons contrasted with the ease of recording expiratory units in this region with extracellular microelectrodes. The difficulty of impalement (and intracellular labeling) was due to the small size of the cell bodies (diameter, 19.6 ± 5.4 μm, mean ± S.D.). The same factor made it necessary to accept recordings from neurons displaying relatively low membrane potentials. It is possible that Zheng et al. ('91b) labeled only expiratory motoneurons in this region because they did not attempt to label neurons with a membrane potential less negative than −40 mV, whereas many of the impaled neurons in the present study had membrane potentials between −30 and −40 mV.

The location of BOT neurons examined in our study closely corresponds to the coordinates of recordings made in the rat by Ezure et al. ('88) and Zheng et al. ('91a). However, in those studies no distinction could be made between recordings from motoneurons and interneurons (see above). This was also the case for recordings obtained in our study from neurons which were impaled but not labeled, and which did not respond antidromically following spinal stimuli. For this reason, the remaining part of the Discussion is based on data obtained from the 12 labeled neurons which were positively confirmed as interneurons. Most of these neurons (n = 9) were located ventral or ventromedial to the compact formation. However, some (n = 3) were located more caudally (1.3 to 1.5 mm rostral to the obex), near the caudal end of the semicompact formation (Bieger and Hopkins, '87). These caudal cells may lie within the pre-Bötzinger Complex, a region which has been suggested to be involved in respiratory rhythmogenesis in neonatal rats (Smith et al., '91). As further studies are needed to establish the rostrocaudal extent of the pre-Bötzinger Complex in the adult rat, we have tentatively classified these three caudal neurons as BOT neurons.

Maps of the distribution of expiratory BOT neurons in the transverse plane are available for the cat (Merrill et al., '83; Fedorko and Merrill, '84; Otake et al., '87). Although our reconstructions were made in the parasagittal plane, so that the location of the cell bodies in relation to the compact formation (retrofacial nucleus) cannot be compared directly, our data indicate that the BOT neurons in the rat extend deeper than those of the cat (see also Ezure et al., '88). Therefore, there might be a greater spatial overlap between BOT and subretrofacial (presympathetic) neurons in the rat than in the cat (cf. Pilowsky et al., '90).

Electrophysiology and spinal projections. Like the previous extra- and intracellular data obtained from cats (Ezure, '90) and rats (Ezure et al., '88; Zheng et al., '91a), our study showed that BOT expiratory neurons in the rat form a heterogeneous population. These neurons were classified into three categories, E-AUG, E-DEC, and E-CON, on the basis of their firing pattern and/or the trajectories of their membrane potentials. As mentioned in Results, some E-DEC neurons showed a decrementing firing pattern before spike inactivation, but a constant level of membrane potential after inactivation. It is thus possible that some neurons which inactivated immediately after impalement and then had a constant membrane potential might have had an E-DEC firing pattern before inactivation. Nevertheless, they were still classified as E-CON. A similar problem regarding classification of E-DEC and E-CON neurons was reported for findings obtained from cats (Otake et al., '87; Bianchi et al., '88; Manabe and Ezure, '88). In an extracellular study conducted in rats (Ezure et al., '88), a category of expiratory neurons was denoted E-OTHER (in addition to E-AUG and E-DEC categories), which appears to correspond to our E-CON category.

The relatively low number of E-AUG neurons recorded in the present study (10 of 149 neurons impaled; 3 of 12 neurons labeled) contrasts with data obtained from cats, in which this type of neuron prevails. It is possible that the result could be affected, in the present experiments, by the removal of the modulatory input from lung stretch receptors by vagotomy. In cats, lung inflations inhibit many E-AUG neurons (Kubin and Lipski, '80; Manabe and Ezure, '88) and thus accentuate the augmenting pattern of their firing (at least in artificially ventilated animals with intact vagus nerves, in which the peak of lung inflation often occurs in the early stages of expiration). If the inhibitory effect of afferent input from lung stretch receptors on E-AUG cells is pronounced in rats with intact vagus nerves, vagotomy could be responsible for the relatively low number of E-AUG neurons reported in the present study. However, a relatively low proportion of rostral E-AUG neurons was also found in the extracellular study of Ezure et al. ('88), conducted in nonvagotomised animals, which suggests that the inhibitory effect of lung inflations on these neurons is not strong. It has also been shown that lung inflations facilitate the firing of E-DEC neurons and contribute to the formation of their decrementing firing pattern (Manabe and Ezure, '88). In addition, the E-DEC firing pattern of some neurons could be altered to a plateau firing pattern after changes in the end-expiratory load (Manabe and Ezure, '88). Taking into account these effects of lung-related vagal afferents on the activity of E-AUG and E-DEC neurons, the absence of this modulatory influence in vagotomised animals could result in a large proportion of expiratory BOT neurons showing less sharply accentuated augmenting or decrementing firing patterns.

The membrane potentials recorded in our sample of BOT neurons were generally low. It is not known whether our measurements reflect the true value of the membrane potential or are a consequence of damage from impalement. The latter is likely, due to the small size of the neurons (average axis about 20 μm) and thus it is possible that voltage-sensitive membrane currents have affected the pattern of membrane trajectory or firing, and thus our classification. As the degree of this effect cannot be assessed without voltage clamping, we suggest that in future intracellular studies, classification should be based not only on trajectories of the membrane potential (or firing pattern), but also on other criteria such as responses to lung inflation in nonvagotomised animals.

Another property unevenly represented in different categories of BOT expiratory neurons is the presence of axonal projections to the spinal cord. In the cat, most E-AUG neurons could be antidromically excited following stimuli applied to the cervical segments of the spinal cord, while no E-DEC neurons responded to such stimuli (Fedorko and Lipski, '81; Fedorko and Merrill, '84; Manabe and Ezure, '88). In the present study, electrophysiological evidence for spinal projection was obtained for only three of the 12 BOT neurons, two of which were E-CON and one E-AUG. In addition, one E-AUG neuron which was not tested for antidromic response showed a stem axon projecting to the caudal edge of the section (approximately 0.5 mm caudal to

the obex, Fig. 3A). It is not clear whether the differences between the proportions of spinally projecting axons in our material and those reported in cats (see also Onai and Miura, '86) are due to the small sample size in the present study or to interspecies variation. It should be noted that a large proportion of bulbospinal neurons in the BOT region was found not only in the cat, but also in the rabbit (Ellenberger et al., '90b).

The presence of both propriobulbar and bulbospinal neurons was reported in two studies in rats in which retrograde tracers were used to examine spinal and medullary projections of neurons in the ventrolateral medulla (Ellenberger and Feldman, '90; Núñez-Abades et al., '91). Although the functional identity of the labeled neurons could not be inferred from these anatomical findings, it is possible that at least some belonged to the VRG and BOT groups. Interestingly, both these studies (Ellenberger and Feldman, '90; Núñez-Abades et al., '91) reported a predominance of propriobulbar over bulbospinal neurons at a level more than 1 mm rostral to the obex.

Axonal projections within the medulla and possible synaptic targets. All 12 reconstructed BOT neurons revealed extensive axonal arborisations within the ipsilateral medulla oblongata. In addition, some projected contralaterally. In all three E-AUG neurons, a stem axon bifurcated into a branch which coursed dorsomedially towards the midline, and a descending branch which issued a number of collaterals at various rostrocaudal levels of the nucleus ambiguus. Several distinct collaterals were also traced near the parent cell body. This projection pattern is similar to that described for E-AUG neurons in the cat on the basis of both electrophysiological and anatomical studies (e.g., Bianchi and Barillot, '82; Fedorko and Merrill, '84; Otake et al., '87; Jiang and Lipski, '90).

E-DEC and E-CON cells showed less consistency in the projection pattern of their axons than E-AUG neurons. Although all had caudal projections, some (one E-DEC and all six E-CON) projected rostrally towards the facial nucleus, and there was much variation in the dorsomedial projections of these neurons. Although two previous studies have examined the morphology of E-DEC and E-CON neurons in the region of the BOT in rats (Pilowsky et al., '90; Zheng et al., '91b), only one E-DEC interneuron has been reported (Pilowsky et al., '90); the remainder have been motoneurons. In the only morphological study on these neurons in cats (Otake et al., '87), all four E-CON neurons labeled were motoneurons. Other studies used antidromic mapping of E-DEC and E-CON neurons in cats (Bianchi and Barillot, '82; Manabe and Ezure, '88) and have shown that these neurons have extensive axonal arborisations in the medulla, including projections to the ipsilateral regions of the BOT and caudal and rostral VRG, a finding confirmed by our morphological study in the rat.

The distribution of the boutons of the BOT expiratory neurons labeled in our study parallels that of the axonal arborisations. Boutons were clustered in four rostrocaudal regions: the BOT, the rostral VRG, the caudal VRG, and to a lesser extent, rostral to the BOT at the level of the facial nucleus. Apart from the most rostral peak, due mainly to one E-CON neuron, this distribution parallels that of E-AUG neurons in the cat (Otake et al., '87). The ratio for all eight BOT neurons examined of boutons en passant to boutons terminaux was 1.95 ± 0.56, similar (no significant difference, t-test, $P < 0.05$) to that for E-AUG neurons in cats (2.03 ± 0.37, mean $\pm$ S.D., n = 4, Otake et al., '87).

Close appositions between bouton-like structures of the axons of BOT neurons and the dendrites or cell bodies of labeled inspiratory neurons in the rostral VRG were not found in any of the five cases examined. Although such appositions do not neccessarily indicate synaptic contacts (for discussion see, e.g., Pilowsky et al., '92), the fact that they were not found in our limited sample indicates that synaptic contacts are likely to be infrequent. Such contacts are also unlikely to be identified at the electron microscopic level, unless the degree of staining of presynaptic boutons was inadequate for their visualization at the light microscopic level (a suggestion not supported by the generally good staining of bouton-like axonal varicosities in our material). This lack of appositions was surprising in view of the extensive literature on a monosynaptic inhibitory input from both augmenting and decrementing expiratory neurons of the BOT to inspiratory neurons of the rostral VRG in the cat (e.g., Ezure and Manabe, '88; Fedorko et al., '89; Jiang and Lipski, '90). The interpretation of our negative finding is not clear. It could be due to the small number of pairs examined, or because the examined expiratory neurons have synaptic targets other than those reported in the cat. It should be noted that we did not succeed in simultaneous staining of pairs consisting of an E-AUG neuron and an inspiratory motoneuron or bulbospinal neuron, and thus it is possible that E-AUG neurons make synaptic contacts with inspiratory neurons also in the rat.

In conclusion, our results demonstrate that some features of BOT expiratory neurons in the rat are similar to those previously described in the cat. This mainly relates to their patterns of axonal projection within the medulla and the rostrocaudal distribution of bouton-like structures. However, some properties appear to be different. This includes the relative paucity of E-AUG neurons (at least in vagotomised rats) and of BOT neurons with spinally projecting axons. Furthermore, several labeled BOT neurons in our study did not appear to form synaptic contacts with inspiratory neurons in the rostral VRG, a finding inconsistent with previous electrophysiological studies in the cat in which such (inhibitory) contacts were identified. In addition, our study confirms a previous observation (Zheng et al., '91b) that neurons which were not antidromically activated by stimulation of the cervical portion of the vagus nerves, superior laryngeal nerves, or spinal cord, were frequently found to be motoneurons. Thus it is not possible to distinguish between local motoneurons and true BOT neurons using conventional extra- or intracellular recordings with antidromic stimulation at these three sites. A distinction can only be made on the basis of cell morphology following intracellular labeling (as in our study), or after antidromic testing with microstimulation in the ipsi- and/or contralateral medullary regions to which the BOT neurons project.

Further studies are needed to identify synaptic targets of different types of BOT expiratory neurons in the rat in order to reveal their functional role in the network of brainstem neurons.

ACKNOWLEDGMENTS

We thank Mr. R. Kanjhan and Miss V. Yardley for their excellent technical assistance, and Dr. K. Ezure for his comments on the manuscript. This work was supported by a grant from the Health Research Council of New Zealand.

LITERATURE CITED

Anders, K., D. Ballantyne, A.M. Bischoff, P.M. Lalley, and D.W. Richter (1991) Inhibition of caudal medullary expiratory neurones by retrofacial inspiratory neurones in the cat. J. Physiol. *437:*1–25.

Bianchi, A.L., and J.C. Barillot (1982) Respiratory neurons in the region of the retrofacial nucleus: Pontile, medullary, spinal and vagal projections. Neurosci. Lett. *31:*277–282.

Bianchi, A.L., L. Grélot, S. Iscoe, and L.E. Remmers (1988) Electrophysiological properties of rostral medullary respiratory neurones in the cat: An intracellular study. J. Physiol., Lond. *407:*293–310.

Bieger, D., and D. Hopkins (1987) Viscerotopic representation of the upper alimentary tract in the medulla oblongata in the rat: The nucleus ambiguus. J. Comp. Neurol. *262:*546–562.

Bongianni, F., M. Corda, G. Fontana, and T. Pantaleo (1988) Influences of superior laryngeal afferent stimulation on expiratory activity in cats. J. Appl. Physiol. *65:*385–392.

Cameron, W.E., D.B. Averill, and A.J. Berger (1985) Quantitative analysis of the dendrites of cat phrenic motoneurons stained intracellularly with horseradish peroxidase. J. Comp. Neurol. *230:*91–101.

Chalmers, J.P., and P. Pilowsky (1991) Brainstem and bulbospinal neurotransmitter systems in the control of blood pressure. J. Hypert. *9:*675–694.

Chang, F.-C. (1992) Modification of medullary respiratory-related discharge patterns by behaviours and states of arousal. Brain Res. *571:*281–292.

Dampney, R.A.L. (1993) The subretrofacial vasomotor nucleus: Anatomical, chemical and pharmacological properties, and role in cardiovascular regulation. Prog. Neurobiol. (in press).

Dick, T.E., and A.J. Berger (1985) Axonal projections of single bulbospinal inspiratory neurons revealed by spike-triggered averaging and antidromic activation. J. Neurophysiol. *53:*1590–1603.

Ellenberger, H.H., and J.L. Feldman (1990) Subnuclear organization of the lateral tegmental field of the rat. I. Nucleus ambiguus and ventral respiratory group. J. Comp. Neurol. *294:*202–211.

Ellenberger, H.H., J.L. Feldman, and W.-Z. Zhan (1990a) Subnuclear organization of the lateral tegmental field of the rat. II:Catecholamine neurons and ventral respiratory group. J. Comp. Neurol. *294:*212–222.

Ellenberger, H.H., P.L. Vera, J.R. Haselton, C.L. Haselton, and N. Schneiderman (1990b) Brainstem projections to the phrenic nucleus: An anterograde and retrograde HRP study in the rabbit. Brain Res. Bull. *24:*163–174.

Ezure, K. (1990) Synaptic connections between medullary respiratory neurons and consideration on the genesis of respiratory rhythm. Prog. Neurobiol. *35:*429–450.

Ezure, K., and M. Manabe (1988) Decrementing expiratory neurons of the Bötzinger complex. II. Direct inhibitory synaptic linkage with ventral respiratory group neurons. Exp. Brain Res. *72:*159–166.

Ezure, K., and M. Manabe (1989) Monosynaptic excitation of medullary inspiratory neurons by bulbospinal inspiratory neurons of the ventral respiratory group in the cat. Exp. Brain. Res. *74:*501–511.

Ezure, K., M. Manabe, and H. Yamada (1988) Distribution of medullary respiratory neurons in the rat. Brain Res. *455:*262–270.

Ezure, K., M. Manabe, and K. Otake (1989) Excitation and inhibition of medullary respiratory neurons by two types of burst inspiratory neurons in the cat. Neurosci. Lett. *104:*303–308.

Fedorko, L., and J. Lipski (1981) Axonal projections of the rostral medullary expiratory neurones studied by antidromic activation. Neurosci. Lett. (Suppl). *7:*S206.

Fedorko, L., and E.G. Merrill (1984) Axonal projections from the rostral expiratory neurones of the Bötzinger complex to medulla and spinal cord in the cat. J. Physiol. Lond. *350:*487–496.

Fedorko, L., J. Duffin, and S. England (1989) Inhibition of inspiratory neurons of the nucleus retroambigualis by expiratory neurons of the Bötzinger complex in the cat. Exp. Neurol. *106:*74–77.

Feldman, J.L. (1986) Neurophysiology of breathing in mammals. In: F.E. Bloom (Ed.) Handbook of Physiology, Sect. 1, *The Nervous System*, Vol. IV. Bethesda, MD: American Physiol. Soc. pp. 463–524.

Feldman, J.L., and H.H. Ellenberger (1988) Central coordination of respiratory and cardiovascular control in mammals. Ann. Rev. Physiol. *50:*593–606.

Fukuda, H., and T. Koga (1991) The Bötzinger complex as the pattern generator for retching and vomiting in the dog. Neurosci. Res. *14:*471–485.

Grace, A.A., and R. Llinás (1985) Morphological artefacts induced in intracellularly stained neurons by dehydration: Circumvention using rapid dimethyl sulfoxide clearing. Neuroscience *16:*461–475.

Grélot, L., and A.L. Bianchi (1987) Differential effects of halothane anesthesia on the pattern of discharge of inspiratory and expiratory neurons in the region of the retrofacial nucleus. Brain Res. *404:*335–338.

Grélot, L., A.L. Bianchi, S. Iscoe, and J.E. Remmers (1988) Expiratory neurones of the rostral medulla: anatomical and functional correlates. Neurosci. Lett. *89:*140–145.

Grélot, L., J.C. Barillot, and A.L. Bianchi (1989) Pharyngeal motoneurons: Respiratory related activity and responses to laryngeal afferents in the decerebrate cat. Exp. Brain Res. *78:*336–344.

Guyenet, P.G. (1990) Role of the ventral medulla oblongata in blood pressure regulation. In K.M. Spyer and A.D. Loewy (eds): Central Regulation of Autonomic Functions. New York: Oxford University Press pp. 145–167.

Hinrichsen, C.F.L., and A.T. Ryan (1981) Localization of laryngeal motoneurons in the rat: Morphological evidence for dual innervation. Exp. Neurol. *74:*341–355.

Horikawa, K., and W.E. Armstrong (1988) A versatile means of intracellular labeling: Injection of biocytin and its detection with avidin conjugates. J. Neurosci. Meth. *25:*1–11.

Jacquin, M.F., J.W. Hu, B.J. Sessle, W.E. Renehan, and P.M.E. Waite (1992) Intra-axonal neurobiotin injection rapidly stains the long-range projections of identified trigeminal primary afferents in vivo: Comparisons with HRP and PHA-L. J. Neurosci. Meth. *45:*71–86.

Jiang, C., and J. Lipski (1990) Extensive monosynaptic inhibition of ventral respiratory group neurons by augmenting neurons in the Bötzinger complex in the cat. Exp. Brain Res. *81:*631–648.

Kalia, M.P. (1981) Anatomical organization of central respiratory neurons. Ann. Rev. Physiol. *43:*105–120.

Kalia, M., and M. Mesulam (1980) Brain stem projections of sensory and motor components of the vagus complex in the cat: II. Laryngeal, tracheobronchial, pulmonary, cardiac and gastrointestinal branches. J. Comp. Neurol. *193:*467–508.

Kalia, M., J.L. Feldman, and M.I. Cohen (1979) Afferent projections to inspiratory neuronal region of the ventrolateral nucleus of the tractus solitarius in the cat. Brain Res. *171:*135–141.

Kawaguchi, Y., C.J. Wilson, and P.C. Emson (1990) Intracellular recording of identified neostriatal patch and matrix spiny cells in a slice preparation preserving cortical inputs. J. Neurophysiol. *62:*1052–1068.

Kubin, L., and J. Lipski (1980). Properties of the rostral NRA expiratory group neurons projecting to the contralateral NTS group. Neurosci. Lett. (Suppl) *5:*S141.

Li, Y.-W., Z.J. Gieroba, R.M. McAllen, and W.W. Blessing (1991) Neurons in rabbit caudal ventrolateral medulla inhibit bulbospinal barosensitive neurons in rostral medulla. Am. J. Physiol. (Reg. Int. Comp. Physiol.) *261:*R44–R51.

Lindsey, B.G., L.S. Segers, and R. Shannon (1987) Functional associations among simultaneously monitored lateral medullary respiratory neurons in the cat. II. Evidence for inhibitory actions of expiratory neurons. J. Neurophysiol. *57:*1101–1117.

Lipski, J., and E.G. Merrill (1980) Electrophysiological demonstration of the projection from expiratory neurons in the rostral medulla to contralateral dorsal respiratory group. Brain Res. *197:*521–524.

Lipski, J., A. Trzebski, J. Chodobska, and P. Kruk (1984) Effects of carotid chemoreceptor excitation on medullary expiratory neurons in cats. Respir. Physiol. *57:*279–291.

Lipski, J., C. Barton, D. de Castro, C. Jiang, I. Llewellyn-Smith, G.S. Mitchell, P.M. Pilowsky, M.D. Voss, and H.J. Waldvogel (1993) Neurotransmitter content of respiratory neurons and their inputs: double-labeling studies using intracellular tracers and immunohistochemistry. In D.F. Speck, M.S. Dekin, W.R. Revelette, and D.T. Frazier (eds): Respiratory Control: Central and Peripheral Mechanisms. Lexington: University Press of Kentucky, pp. 62–65.

Long, S., and J. Duffin (1986) The neuronal determinants of respiratory rhythm. Prog. Neurobiol. *27:*101–182.

Manabe, M., and K. Ezure (1988) Decrementing expiratory neurons of the Bötzinger complex. I. Response to lung inflation and axonal projection. Exp. Brain Res. *72:*150–158.

Mateika, J.H., and J. Duffin (1989) The connections from Bötzinger expiratory neurons to upper cervical inspiratory neurons in the cat. Exp. Neurol. *104:*138–146.

Merrill, E.G., and L. Fedorko (1984) Monosynaptic inhibition of phrenic motoneurons: A long descending projection from Bötzinger neurons. J. Neurosci. *4:*2350–2353.

Merrill, E.G., J. Lipski, L. Kubin, and L. Fedorko (1983) Origin of the expiratory inhibition of the nucleus tractus solitarius inspiratory neurones. Brain Res. *263:*43–50.

Miller, A.D., and S. Nonaka (1990) Bötzinger expiratory neurons may inhibit phrenic motoneurons and medullary inspiratory neurons during vomiting. Brain Res. *521:*352–354.

Morgan, C.W., W.C. de Groat, L.A. Felkins, and S.J. Zhang (1991) Axon collaterals indicate broad intraspinal role for sacral preganglionic neurons. Proc. Natl. Acad. Sci. USA. *88:*6888–6892.

Núñez-Abades, P.A., R. Pásaro, and A.L. Bianchi (1991) Localization of respiratory bulbospinal and propriobulbar neurons the region of the nucleus ambiguus of the rat. Brain Res. *568:*165–172.

Onai, T., and M. Miura (1986) Projections of supraspinal structures to the phrenic motor nucleus in cats studied by a horseradish peroxidase microinjection method. J. Aut. Nerv. Syst. *16:*61–77.

Orem, J., and E.G. Brooks (1986) The activity of retrofacial expiratory cells during behavioural respiratory responses and active expiration. Brain Res. *374:*409–412.

Otake, K., H. Sasaki, H. Mannen, and K. Ezure (1987) Morphology of expiratory neurons of the Bötzinger complex: An HRP study in the cat. J. Comp. Neurol. *258:*565–579.

Otake, K., H. Sasaki, K. Ezure, and M. Manabe (1988) Axonal projection from Bötzinger expiratory neurons to contralateral ventral and dorsal respiratory groups in the cat. Exp. Brain Res. *72:*167–177.

Otake, K., H. Sasaki, K. Ezure, and M. Manabe (1990) Medullary projection of non-augmenting respiratory neurons of the ventrolateral medulla in the cat. J. Comp. Neurol. *302:*485–499.

Pantaleo, T., and M. Corda (1985) Expiration-related neurons in the region of the retrofacial nucleus: Vagal and laryngeal inhibitory influences. Brain Res. *359:*343–346.

Pilowsky, P.M., C. Jiang, and J. Lipski (1990) An intracellular study of respiratory neurons in the rostral ventrolateral medulla of the rat and their relationship to catecholamine-containing neurons. J. Comp. Neurol. *301:*604–617.

Pilowsky, P., J.J. Llwellyn-Smith, J. Lipski, and J. Chalmers (1992) Sub-stance P immunoreactive boutons form synapses with feline sympathetic preganglionic neurons. J. Comp. Neurol. *320:*121–135.

Richter, D.W., and D. Ballantyne (1988) On the significance of post-inspiration. In: J. Grote (ed) *Funktionsanalyse Biologischer Systeme.* Stuttgart, New York: Gustav Fischer Vrg, pp. 149–156.

Schwarzacher, S.W., Z. Wilhelm, K. Anders, and D.W. Richter (1991) The medullary respiratory network in the rat. J. Physiol. Lond. *435:*631–644.

Shannon, R., and B.G. Lindsey (1987) Expiratory neurons in the region of the retrofacial nucleus: Inhibitory effects of intercostal tendon organs. Exp. Neurol. *97:*730–734.

Smith, J.C., H.H. Ellenberger, K. Ballanyi, D.W. Richter, and J.L. Feldman (1991) Pre-Bötzinger Complex: A brainstem region that may generate respiratory rhythm in mammals. Science *254:*725–729.

Smith, J.C., D.E. Morrison, H.H. Ellenberger, M.R. Otto, and J.L. Feldman (1989) Brainstem projections to the major respiratory neuron populations in the medulla of the cat. J. Comp. Neurol. *281:*69–96.

Speck, D.F. (1989) Bötzinger complex region role in phrenic-to-phrenic inhibitory reflex of cat. J. Appl. Physiol. *67:*1364–1370.

St. John, W.M., Q. Hwang, E.E. Nattie, and D. Zhou (1989) Functions of the retrofacial nucleus in chemosensitivity and ventilatory neurogenesis. Resp. Physiol. *76:*159–172.

Zheng, Y., J.C. Barillot, and A.L. Bianchi (1991a) Patterns of membrane potentials and distributions of the medullary respiratory neurons in the decerebrate rat. Brain Res. *546:*261–270.

Zheng, Y., J.C. Barillot, and A.L. Bianchi (1991b) Are the post-inspiratory neurons in the decerebrate rat cranial motoneurons or interneurons? Brain Res. *551:*256–266.

Zheng, Y., J.C. Barillot, and A.L. Bianchi (1992) Medullary expiratory neurons in the decerebrate rat; an intracellular study. Brain Res. *576:*245–253.